The North Atlantic Oscillation as a driver of Northern Hemisphere rapid climate change

Thomas L. Delworth, Fanrong Zeng, Gabriel A. Vecchi, Xiaosong Yang, Liping Zhang, and Rong Zhang
Geophysical Fluid Dynamics Laboratory/NOAA
201 Forrestal Rd.
Princeton, NJ 08540 USA

Revised version submitted to Nature Geoscience
May 10, 2016

Dramatic climate changes have occurred since the 1970s, including rapid loss of Arctic sea ice[1], large-scale warming[2], and increased tropical storm activity[3] in the Atlantic. Anthropogenic radiative forcing has likely played a major role in these changes[4], but the relative influence of anthropogenic forcing and natural variability is not well established. The above changes have also occurred during a period in which the North Atlantic Oscillation has shown marked multidecadal variations[5]. Here we investigate the role of the North Atlantic Oscillation in these rapid changes through its' influence on the Atlantic Meridional Overturning Circulation and ocean heat transport. We use climate models to show that observed multidecadal variations of the North Atlantic Oscillation can induce multidecadal variations in the Atlantic Meridional Overturning Circulation and poleward ocean heat transport in the Atlantic, extending to the Arctic. Our results suggest that these variations have contributed to the rapid loss of Arctic sea, Northern Hemisphere warming, and changing Atlantic tropical storm activity, especially in the late 1990s and early 2000s. These multidecadal variations are superimposed on long-term anthropogenic forcing trends that are the dominant factor in long-term Arctic sea ice loss and hemispheric warming.

There has been pronounced multidecadal variability of the North Atlantic Oscillation (NAO) over the last century[6], with a negative phase of the NAO from the 1960s into the 1970s (Fig. 1a), associated with weakened westerly winds and cold ocean surface temperatures in the subpolar North Atlantic. This was followed by a rapid switch to a positive NAO phase from the 1980s into the early 2000s, along with strengthened westerly winds and rapid warming in the subpolar North Atlantic. These regional variations were coincident with long-term trends and multidecadal variability in NH surface air temperature[2] and Arctic sea ice[1]. The relatively cool period of the 1970s was coincident with enhanced Arctic sea ice[7], although observations prior to the satellite era are uncertain. This was followed by a rapid warming of the Northern Hemisphere (NH) and reduction of Arctic sea ice from the late 1970s through the 2000s. There have been substantial multidecadal variations in Atlantic tropical storm activity[3], with a relatively quiescent period from the late 1960s through the 1980s, followed by enhanced activity after the mid 1990s.

Studies have suggested an important role for anthropogenic forcing in driving some of the above changes[4,8], and yet the relative roles of natural variability and anthropogenic forcing are uncertain. In particular, the degree to which natural climate variability contributes to these past variations is a critical factor in our confidence in projections of future climate.

We use simulations with three different climate models to explore the contribution of multidecadal variations of the NAO to the above changes. The novel experimental design (see Methods) adds NAO related surface heat flux anomalies into the ocean component of coupled models, thereby allowing an assessment of the response of the climate system to these NAO variations. Our results show that observed multidecadal NAO variations induce variations in Atlantic Ocean heat transport, primarily associated with the Atlantic Meridional Overturning Circulation (AMOC), that can contribute to recently observed rapid Arctic sea ice loss, extratropical NH warming, and decadal-scale changes in Atlantic tropical storm activity.

We use ensembles of simulations that cover the period 1951-2015. In the first suite of simulations (labeled "HIST") we incorporate historical estimates of changing radiative forcing from human and natural sources, including greenhouse gases, aerosols, ozone, solar irradiance and volcanic aerosols. In the second set (labeled "HIST+NAO") we include these same forcings, but add to the model ocean an additional pattern of air-sea heat flux that corresponds to a positive phase of the NAO (see Supplementary Figure S1). We multiply the pattern of extra heat flux forcing by the observed value of the NAO index for that year (Fig. 1a). Differences between the sets of experiments (HIST+NAO minus HIST) provide an estimate of the impact of the observed time-varying NAO on the North Atlantic Ocean and global climate system. We use three climate models for robustness.

Idealized experiments have revealed a profound influence of the NAO on the AMOC[10,11]. A positive phase of the NAO is characterized by enhanced westerly winds across the middle latitudes of the North Atlantic (see schematic in Supplementary Figure S2). During winter these strengthened winds bring colder, drier air from the North American continent over the warmer ocean[5], thereby enhancing air-sea temperature differences that lead to an increased flux of heat from the ocean to the atmosphere in the Labrador Sea and subpolar region of the North Atlantic. This leads to colder, denser water in the upper ocean and enhanced deepwater formation in the Labrador Sea region[12]. In idealized simulations the increased upper ocean density in the western part of the subpolar gyre creates a zonal density gradient that leads to enhanced northward flow in the upper ocean and a strengthening of the AMOC after a lag of five to ten years[13]. The strengthened AMOC transports more heat poleward, leading to high-latitude warming and climatic impacts. The resulting temperature response is superficially counter-intuitive, with some of the largest surface ocean warming in the subpolar region where the prescribed perturbations act to remove heat from the ocean (compare Figures 1a and 9a in Delworth and Zeng, 2015). This can only be understood by accounting for the changing transport of heat by the ocean circulation.

Time series of the observed NAO and its simulated impact on the Atlantic are shown in Figure 1. The NAO transitions from a negative phase (weakened westerly winds) in the 1960s to a strong positive phase (strengthened westerly winds) in the 1980s and 1990s (Fig. 1a), with some return to more neutral conditions after 2000. The simulated AMOC (Fig. 1b) responds to these NAO variations, and transitions from a weakened state in the 1960s and early 1970s to a strengthened state in the 1990s, with gradual weakening after 2000. The AMOC changes are mirrored by variations in northward ocean heat transport in the subpolar North Atlantic (Fig. 1c) as well as heat transport into the Barents Sea and Arctic (Fig. 1d).

The variations in poleward ocean heat transport influence Arctic sea ice[14,15] and large-scale climate. In particular, enhanced Atlantic heat transport into the Arctic can lead to net basal melting and a reduction of Arctic ice mass in all seasons, resulting in reduction of winter and summer Arctic sea ice extent on multidecadal time scales[16]. We show in Figure 2 the time series of changes in observed and simulated areal extent of Arctic sea ice for both March and September, as well as the linear trends over 1979-2005. The NAO variations lead to an enhancement of Arctic sea ice extent in the 1960s and 1970s[7] in response to reduced ocean heat transport into the Arctic, and a reduction in sea ice extent in the 1980s through 2015 associated with enhanced ocean heat transport into the Arctic. The rate of simulated sea ice reduction (1979-2005) is greater when the NAO forcing is included (insets in Figure 2a and 2c). The NAO impacts are similar in both seasons, but their relative impact as a fraction of the observed change is larger in winter due to the smaller observed trends in winter (spatial patterns shown in Supplementary Figure S3). These results suggest that NAO-induced ocean heat transport variations may have contributed to the rapid loss of Arctic sea ice in the 1990s and early 2000s, especially during winter, and therefore augmented the decline due to anthropogenic radiative forcing. In these simulations the NAO effect was strongest in the 1990s and early 2000s, but has weakened after approximately 2005, consistent with the decline of the NAO from peak values in the 1990s.

The variations in poleward ocean heat transport and Arctic sea ice also impact surface air temperature over the NH extratropics[17] (Figure 3, and Supplementary Figure S4). The weakened AMOC in the 1960s and 1970s led to a simulated extratropical NH cooling of 0.1-0.2K, followed by a strengthening AMOC leading to a simulated extratropical NH warming of ~0.2K by the year 2000. This warming is driven by enhanced ocean heat transport, but is also amplified by coupled ocean-atmosphere-land-ice feedbacks. The associated reductions in ice extent and snow, including on surrounding continental regions, reduce albedo and increase absorbed shortwave radiation. This provides an important positive feedback that amplifies the warming signal from the ocean heat transport increase.

This simulated large-scale warming of the NH influences large-scale atmospheric circulation, including a reduction in the meridional temperature gradient. This leads to a weakening of upper atmosphere westerly winds in the subtropics over the Atlantic, and a reduction in the vertical shear of the zonal wind (see Supplementary Figures S5 and S6). Since shear is one of the dominant factors influencing tropical storm activity[18], we examine changes in Atlantic tropical storm activity in response to NAO-induced AMOC variations. Only one of the models (FLOR, see Methods) has sufficient atmospheric resolution to credibly simulate aspects of Atlantic tropical storms[19]. We show in Figure 4 the changes in simulated tropical storm activity between 1965-1994 (reduced heat transport in response to the NAO, and larger vertical wind shear) and 1995-2014 (enhanced heat transport and reduced vertical wind shear). The inclusion of the NAO forcing leads to a systematic shift to more frequent tropical storms in the Atlantic in the latter period. The fraction of attributable risk[20] of the change in tropical storm activity to the imposed NAO-related flux forcing is 97%. This suggests that NAO variations could have contributed to the observed increase in Atlantic tropical storm activity in the post 1995 period relative to earlier decades.

Our results demonstrate that multidecadal changes in the NAO can have a broad impact on climate through their influence on poleward ocean heat transport. These changes include modulating Atlantic ocean temperature, Arctic sea ice, NH extratropical temperature, and Atlantic tropical storm activity. This is consistent with model and observational analyses showing substantial Arctic and Atlantic natural variability on multidecadal time scales, and is also consistent with observational analyses showing the importance of ocean circulation for surface heat fluxes[21] and North Atlantic ocean heat content variations[22]. There are a number of uncertainties associated with these results, including details of the observed NAO flux forcing, the models' response to the NAO, and the response of the climate system to ocean heat transport variations, including cloud and shortwave radiation feedbacks. The experiments shown here impose only NAO-related heat flux anomalies. We have conducted additional simulations that also imposed NAO-related wind stress anomalies, and the principal results are similar to those shown here (Supplementary Fig. S7). However, wind stress anomalies are an important factor influencing direct wind-driven AMOC variability, especially at interannual time scales[23]. The current work has demonstrated that NAO-induced AMOC changes could have played a substantial role in observed rapid changes in Arctic sea ice (primarily in winter), extratropical temperature change, and Atlantic tropical storm activity over the last several decades.

This study has implications both for the study of past climates and for projections of future climate. Proxy reconstructions indicate substantial multidecadal variability of the NAO over the past

1000 years and longer[24]. Such NAO variations would have likely altered the AMOC and thereby influenced hemispheric-scale climate as shown in this study, in addition to the direct effect of NAO variations on atmospheric circulation and climate[5]. In addition, decadal predictions made with two of the models used in this study, as well as other models[5], suggest a weakening of the AMOC over the next decade (Supplementary Figure S8). This is consistent with observed changes in the North Atlantic[23,25,26], including the return of the NAO to a more neutral state over the last decade and the projected response to anthropogenic radiative forcing. In isolation, a weakening AMOC would tend to moderate the rate of loss of Arctic sea ice[5] and warming over the NH extratropics through reduced poleward oceanic heat transport. This might also create a tendency towards fewer Atlantic tropical storms, but this effect in a decadal projection is embedded within the considerable variability in the number of simulated tropical storms that arise purely from internal variability.

References

1. Vaughan, D. G. *et al.* in *Climate Change 2013: The Physical Science Basis. Contribution of Working Group 1 to the Fofth Assessment Report of the Intergovernmental Panel on Climate Change.* (Cambridge University Press, Cambridge, United Kingdom and New York, NY, USA., 2013).
2. Hartmann, D. L. *et al.* in *Climate Change 2013: The Physical Science Basis. Contribution of Working Group 1 to the Fofth Assessment Report of the Intergovernmental Panel on Climate Change.* (Cambridge University Press, Cambridge, United Kingdom and New York, NY, USA., 2013).
3. Kossin, J. P. & Vimont, D. J. A More General Framework for Understanding Atlantic Hurricane Variability and Trends. *Bull. Am. Meteorol. Soc.* **88,** 1767–1781 (2007).
4. Bindoff, N.L., et al. *Detection and Attribution of Climate Change: from Global to Regional.* (Cambridge University Press, Cambridge, United Kingdom and New York, NY, USA., 2013).
5. Yeager, S. G., Karspeck, A. & Danabasoglu, G. Predicted slow-down in the rate of Atlantic sea ice loss. *Geophys. Res. Lett.* (2015). doi:10.1002/2015GL065364
6. Li, J., Sun, C. & Jin, F.-F. NAO implicated as a predictor of Northern Hemisphere mean temperature multidecadal variability. *Geophys. Res. Lett.* **40,** 5497–5502 (2013).
7. Miles, M. W. *et al.* A signal of persistent Atlantic multidecadal variability in Arctic sea ice. *Geophys. Res. Lett.* **41,** 463–469 (2014).
8. Gillett, N. P. *et al.* Attribution of polar warming to human influence. *Nat. Geosci.* **1,** 750–754 (2008).
9. Hurrell, J. W. & Deser, C. North Atlantic climate variability: The role of the North Atlantic Oscillation. *J. Mar. Syst.* **78,** 28–41 (2009).
10. Eden, C. & Jung, T. North Atlantic interdecadal variability: oceanic response to the North Atlantic Oscillation (1865-1997). *J. Clim.* **14,** 676–691 (2001).
11. Delworth, T. L. & Zeng, F. The impact of the North Atlantic Oscillation on climate through its influence on the Atlantic Meridional Overturning Circulation. *J. Clim.* **Accepted,** (2015).

12. Danabasoglu, G. *et al.* Variability of the Atlantic Meridional Overturning Circulation in CCSM4. *J. Clim.* **25,** 5153–5172 (2012).

13. Yeager, S. & Danabasoglu, G. The Origins of Late-Twentieth-Century Variations in the Large-Scale North Atlantic Circulation. *J. Clim.* **27,** 3222–3247 (2014).

14. Mahajan, S., Zhang, R. & Delworth, T. L. Impact of the Atlantic Meridional Overturning Circulation (AMOC) on Arctic Surface Air Temperature and Sea Ice Variability. *J. Clim.* **24,** 6573–6581 (2011).

15. Day, J. J., Hargreaves, J. C., Annan, J. D. & Abe-Ouchi, A. Sources of multi-decadal variability in Arctic sea ice extent. *Environ. Res. Lett.* **7,** 034011 (2012).

16. Zhang, R. Mechanisms for low-frequency variability of summer Arctic sea ice extent. *Proc. Natl. Acad. Sci.* **112,** 4570–4575 (2015).

17. Chylek, P. *et al.* Isolating the anthropogenic component of Arctic warming. *Geophys. Res. Lett.* **41,** 3569–3576 (2014).

18. Gray, W. Global view of the origin of tropical disturbances and storms. *Mon. Weather Rev.* **96,** 669–700 (1968).

19. Vecchi, G. A. *et al.* On the Seasonal Forecasting of Regional Tropical Cyclone Activity. *J. Clim.* **27,** 7994–8016 (2014).

20. Stone, D. A. & Allen, M. R. The End-to-End Attribution Problem: From Emissions to Impacts. *Clim. Change* **71,** 303–318 (2005).

21. Gulev, S. K., Latif, M., Keenlyside, N., Park, W. & Koltermann, K. P. North Atlantic Ocean control on surface heat flux on multidecadal timescales. *Nature* **499,** 464–467 (2013).

22. McCarthy, G. D., Haigh, I. D., Hirschi, J. J.-M., Grist, J. P. & Smeed, D. A. Ocean impact on decadal Atlantic climate variability revealed by sea-level observations. *Nature* **521,** 508–510 (2015).

23. Smeed, D. A. *et al.* Observed decline of the Atlantic meridional overturning circulation 2004-2012. *Ocean Sci.* **10,** 29–38 (2014).

24. Ortega, P. *et al.* A model-tested North Atlantic Oscillation reconstruction for the past millennium. *Nature* **523,** 71–74 (2015).

25. Robson, J., Hodson, D., Hawkins, E. & Sutton, R. Atlantic overturning in decline? *Nat. Geosci.* **7,** 2–3 (2014).

26. Hermanson, L. *et al.* Forecast cooling of the Atlantic subpolar gyre and associated impacts. *Geophys. Res. Lett.* **41,** 5167–5174 (2014).

27. Dee, D. P. *et al.* The ERA-Interim reanalysis: configuration and performance of the data assimilation system. *Q. J. R. Meteorol. Soc.* **137,** 553–597 (2011).

28. Delworth, T. L. *et al.* GFDL's CM2 global coupled climate models. Part I: Formulation and simulation characteristics. *J. Clim.* **19,** (2006).

29. Donner, L. J. *et al.* The Dynamical Core, Physical Parameterizations, and Basic Simulation Characteristics of the Atmospheric Component AM3 of the GFDL Global Coupled Model CM3. *J. Clim.* **24,** 3484–3519 (2011).

30. Zhang, S., Harrison, M. J., Rosati, A. & Wittenberg, A. System Design and Evaluation of Coupled Ensemble Data Assimilation for Global Oceanic Climate Studies. *Mon. Weather Rev.* **135,** 3541–3564 (2007).

Acknowledgements

We thank M. Harrison, H, Murakami, and A. Wittenberg for valuable comments on a preliminary version of this manuscript, along with two anonymous reviewers.

Author contributions

T.L.D. designed the study, conducted analyses, and wrote the paper. F. Z. conducted the model simulations, contributed to the analyses. L. Z. conducted analyses of wind shear and decadal predictions. G.A.V. conducted analyses of changes in tropical storm activity, and contributed ideas for analyses and interpretation of results. All helped to improve the manuscript.

Figures

Figure 1 Time series of NAO and associated changes in ocean circulation. (a) Time series of the observed NAO index based on differences in normalized Dec-Mar sea level pressure between Portugal and Iceland (positive values associated with stronger mid-latitude westerly winds). (b) Response of the model AMOC to the NAO flux forcing, calculated as the AMOC in the HIST+NAO simulations minus the AMOC in the HIST simulations. The AMOC index is calculated as the maximum value in depth of the annual mean streamfunction of the flow at 50^{o}N. Units are Sverdrups (Sv; 1 Sv = 10^6 m^3s^{-1}). The diamonds indicate the mean response using all three models. The shaded bars denote the 5-95% confidence interval around the mean response as calculated from resampling the control simulations. (c) Same as (b) for ocean heat transport at 50^{o}N). (d) Same as (b) for ocean heat transport into Barents Sea (calculated as zonal heat transport across a line connecting Norway and Spitsbergen at approximately 10^{o}E; note the different vertical scales in (c) and (d)).

Figure 2 Observed and simulated changes in Arctic sea ice extent. (a) Time series of change in March Arctic sea ice area relative to the 1979-1990 mean (units are 10^{12} m^2; sea ice extent refers to area with sea ice concentration greater than 15%). Blue curve shows the observations (from the National Snow and Ice Data Center; http://nsidc.org/data). The squares show the multi-model mean for HIST+NAO (black) and HIST (red). The colored bars (green for HIST+NAO, tan for HIST) indicate the 5-95% range around the multi-model mean, where the distribution is estimated based on resampling control simulations for each. The grey bars indicate where the tan and green bars overlap. The inset shows the linear trend from 1979 to 2005 of March Arctic sea ice area in observations (black circle), CM2.1 (circles), FLOR (diamonds), and CM3 (squares). Tan (green) symbols are from HIST (HIST+NAO). (b) Difference in ice extent calculated as HIST+NAO minus HIST. The bars indicate the 5-95% range as estimated from resampling the control simulations. (c) Same as (a) for September. (d) Same as (b) for September.

Figure 3 Response of Northern Hemisphere extratropical (23^{o}N-90^{o}N) surface air temperature to NAO heat flux forcing. The diamonds indicate the multi-model ensemble mean difference (HIST+NAO minus HIST). The shading indicates the 5-95% limits around that mean as estimated from resampling the control simulations.

Figure 4 Probability distribution functions of changes in Atlantic tropical cyclone activity for the 1995-2014 period relative to the 1965-1994 period. Values along the x-axis indicate percentage changes in the number of tropical storms for 1995-2014 relative to the number for 1965-1994. The black curve is based on HIST. The fact that the black curve is approximately symmetric around zero indicates that the model simulates no systematic change in tropical storm activity in response to radiative forcing change for the 1995-2014 period relative to the 1965-1994 period. In contrast, the red curve is from HIST+NAO simulations. The fact that the red curve is to the right of the black curve and is not symmetric around zero indicates an enhanced probability of an increase in tropical cyclone activity for the 1995-2014 period relative to the earlier period when NAO forcing is included. The observed change is indicated by the vertical blue line. The PDFs are generated by resampling the numbers of storms each year from the model simulations (see Supplementary Information for details).

Methods

Models

We use three climate models and subject them to identical forcings from NAO related surface flux anomalies. The first model is the Geophysical Fluid Dynamics Laboratory (GFDL) CM2.1 model [28]. This is a fully coupled ocean-atmosphere model, with land and atmospheric resolution of approximately 200 km in the horizontal, and 24 vertical levels in the atmosphere. The ocean component has horizontal resolution of approximately 100 km, with finer resolution in the tropics, and 50 levels in the vertical. This model has been used in a wide variety of studies of climate variability, predictability and change, and extensive model output from past studies is available at http://nomads.gfdl.noaa.gov/CM2.X/ and http://nomads.gfdl.noaa.gov:8080/DataPortal/cmip5.jsp. The second model used is called CM2.5_FLOR[19], referred to here as "FLOR", where "FLOR" stands for Forecast oriented Low Ocean Resolution. This model uses atmospheric physics that are very similar to CM2.1, but has a higher spatial resolution in the atmosphere. The horizontal resolution of the atmosphere and land model is approximately 50 km (versus 200 km in CM2.1). The number of vertical levels in the atmosphere has increased from 24 in CM2.1 to 32 in FLOR. The ocean component of FLOR is similar to that in CM2.1. The third model used is CM3[29]. This has a similar horizontal spatial resolution as CM2.1, but has substantially increased vertical resolution (48 layers), and includes representations of the indirect effect of aerosols and interactive chemistry. As in the other two models, the horizontal resolution of the ocean component is approximately 1°.

Experiments

For each model, simulations over the period 1861-2015 have been conducted in which the model is driven by changing concentrations of atmospheric greenhouse gases, ozone, and aerosols (anthropogenic and volcanic), as well as land use changes and solar irradiance changes. For the period 1861-2005 these are based on observational estimates, while after 2005 they are based on projections using the Radiative Concentration Pathways scenario 4.5 (RCP4.5; see http://cmip-pcmdi.llnl.gov/cmip5/forcing.html for details). For CM3 ozone is directly predicted in the model. For each model we conduct ensembles of simulations starting from widely separated points in a long control simulation. Ensemble sizes are 10, 5, and 5 members for CM2.1, FLOR, and CM3 respectively. We call these experiments "HIST".

A second ensemble of simulations is performed for each model that is identical to the first ensemble described above, except that at each time step an extra pattern of surface heat flux is added to the model ocean. This heat flux has the same spatial signature as the observed NAO, and was derived by computing a linear regression at each grid point between the time series of seasonal mean (Dec-Mar) surface heat flux anomalies from the ECMWF-Interim reanalysis[27] and an observed NAO index (Dec-Mar mean; data obtained from NCAR/UCAR Data Climate Guide at https://climatedataguide.ucar.edu/climate-data/hurrell-north-atlantic-oscillation-nao-index-station-based). This pattern therefore yields the surface heat flux anomaly pattern associated with a unit change in the observed NAO index (the pattern is shown in Extended Data Figure 1). The flux anomalies were added only in the months of December-March, the period of maximum deepwater formation in the North Atlantic The pattern of heat flux anomalies was applied only over the Atlantic north of the Equator, up to and including the Greenland and Barents Seas, but excluding the Arctic. The heat flux anomalies were normalized such that their areal integral is zero. The anomalies therefore do not add or subtract heat from the system; they merely rearrange the surface fluxes consistent with the NAO. The heat flux anomalies added each year are calculated as the regression coefficient multiplied by the observed NAO index that year. We call these experiments "HIST+NAO". Additional experiments were performed that also imposed NAO related wind stress anomalies in addition to heat flux anomalies; the primary results of these experiments are consistent with those using only heat flux anomalies.

We note that the differences between the HIST+NAO experiments and the HIST experiments are primarily attributable to the imposed NAO additional NAO flux anomalies, but we note that each simulation also computes its own internal NAO variability. This internally computed NAO variability acts in addition to the imposed fluxes, and therefore is a source of noise that complicates the interpretation of the results. We have resampled the NAO from long control simulations of each model, and estimate that for these ensemble sizes the 5-95% limits of yearly ensemble mean NAO differences are -0.99 to +0.99. Since our primary results come from extended periods with absolute NAO values greater in one, this analysis suggests that such internal variability is modest compared to the signal from the imposed NAO forcing.

Decadal Prediction

Ten-member ensembles of decadal hindcast/prediction experiments have been conducted using the CM2.1 and FLOR models. In these prediction experiments the models are initialized from the observed state of the climate system as estimated using GFDL's Ensemble Coupled Data Assimilation (ECDA) system[30]. These hindcasts/predictions are initialized on January 1 of each year from 1961 to 2015, and the hindcasts/predictions are run for ten years forward in time from that point. The simulations are forced with estimates of observed changes in radiative forcing from 1861 to 2005, and by estimates of forcing based on the Radiative Concentration Pathways scenario 4.5 (RCP4.5; see http://cmip-pcmdi.llnl.gov/cmip5/forcing.html for details) from 2006 onwards. These prediction experiments provide the basis for the AMOC predictions shown in Supplementary Figure S8.

Data Availability

Source for the observed NAO index: Hurrell, James & National Center for Atmospheric Research Staff (Eds). Last modified 20 Oct 2015. "The Climate Data Guide: Hurrell North Atlantic Oscillation (NAO) Index (station-based)." Retrieved from https://climatedataguide.ucar.edu/climate-data/hurrell-north-atlantic-oscillation-nao-index-station-based. ECMWF-interim reanalysis data[27] downloaded from http://apps.ecmwf.int/datasets/data/interim_full_moda/. Observed sea ice extent obtained from the National Snow and Ice Data Center (http://nsidc.org/data).

Code availability

The source code for the models used in this study is available as follows: CM2.1, http://www.gfdl.noaa.gov/accessing-cm2-1p1; FLOR, http://www.gfdl.noaa.gov/cm2-5-and-flor-quickstart; CM3, Atmospheric component, http://www.gfdl.noaa.gov/am3.

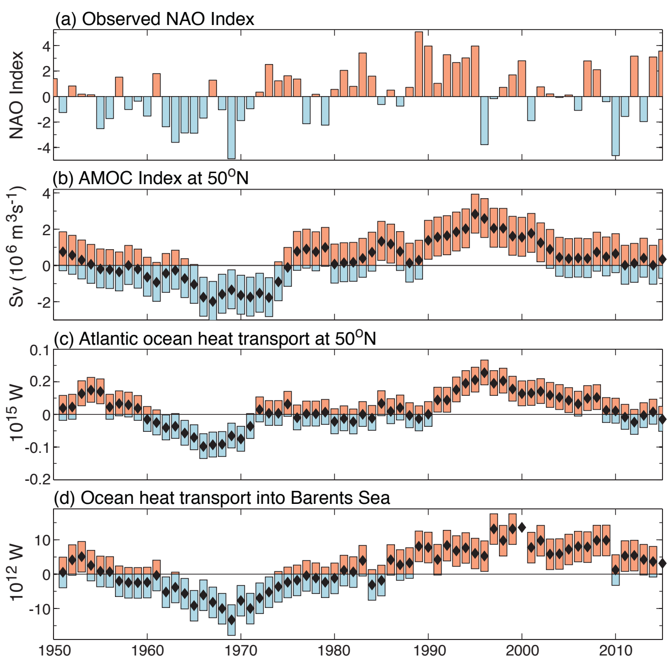

(a) Observed NAO Index
NAO Index
(b) AMOC Index at 50^{o}N
Sv (10^6 m^3s^{-1})
(c) Atlantic ocean heat transport at 50^{o}N
10^{15} W
(d) Ocean heat transport into Barents Sea
10^{12} W
1950
1960
1970
1980
1990
2000
2010

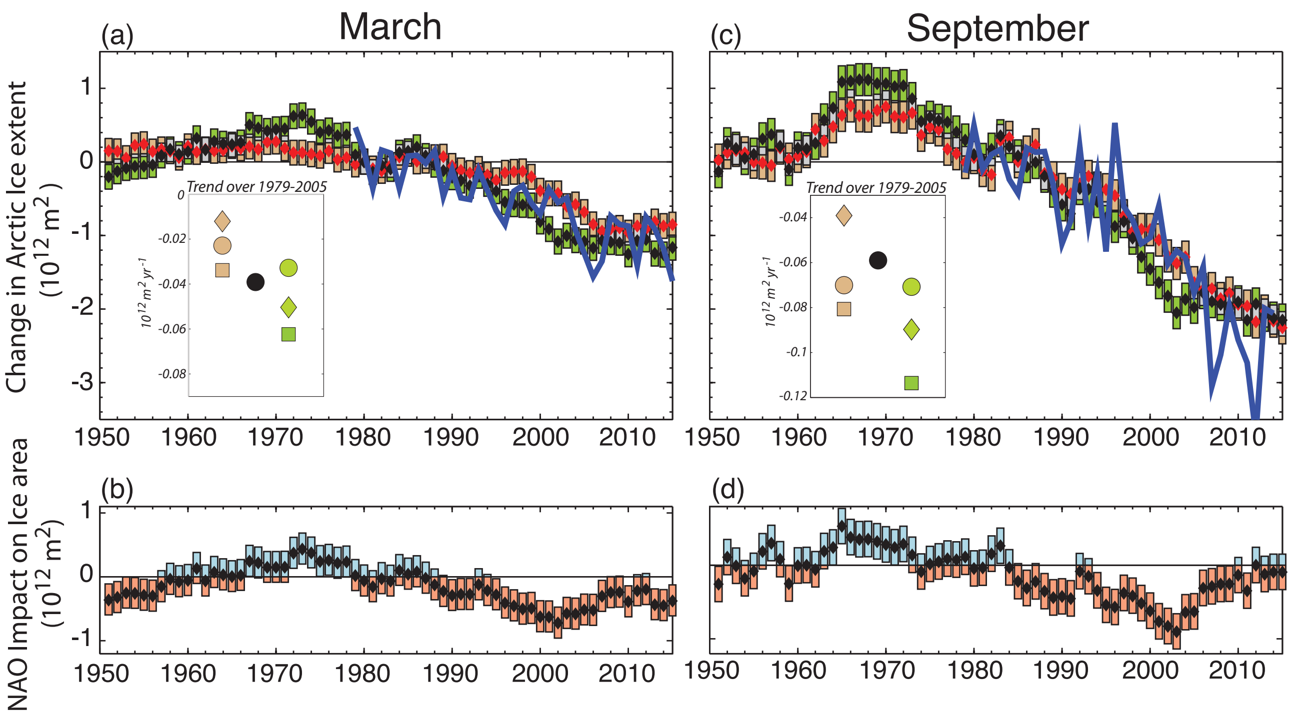

(a)
March
(c)
September
Change in Arctic Ice extent
(10^{12} m^2)
Trend over 1979-2005
10^{12} m^2 yr^{-1}
1
0
-1
-2
-3
0
-0.02
-0.04
-0.06
-0.08
-0.04
-0.06
-0.08
-0.1
-0.12
1950
1960
1970
1980
1990
2000
2010
(b)
(d)
NAO Impact on Ice area
(10^{12} m^2)

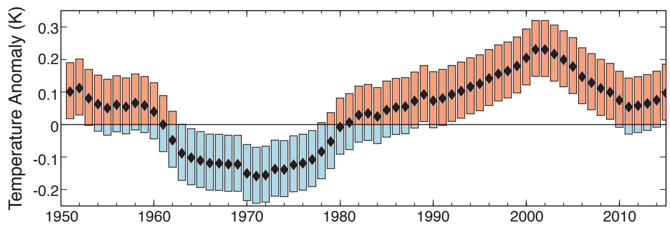

Temperature Anomaly (K)
0.3
0.2
0.1
0
-0.1
-0.2
1950
1960
1970
1980
1990
2000
2010

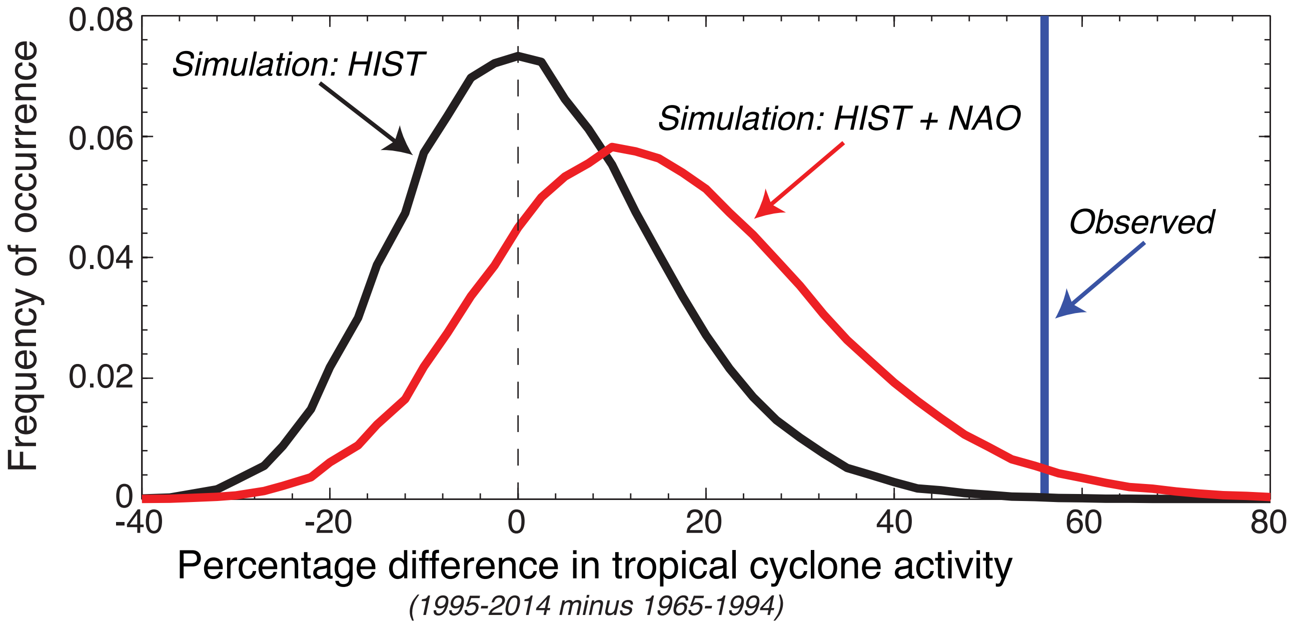
0.08
0.06
0.04
0.02
0
Frequency of occurrence
Simulation: HIST
Simulation: HIST + NAO
Observed
-40
-20
0
20
40
60
80
Percentage difference in tropical cyclone activity
(1995-2014 minus 1965-1994)